Science Bulletin 71 (2026) 1450–1460

Contents lists available at ScienceDirect

Science Bulletin

journal homepage: www.elsevier.com/locate/scib

Article

Impervious surface increase over global border areas regulated by population and topography

Chiwei Xiao [a,b], Zilong Yue [a,b], Zhiming Feng [a,b,*], Yi Wang [a,b], Josep Peñuelas [c], Chaoyang Wu [a,b,*]

[a] Institute of Geographic Sciences and Natural Resources Research, Chinese Academy of Sciences, Beijing 100101, China
[b] College of Resources and Environment, University of Chinese Academy of Sciences, Beijing 100049, China
[c] CSIC, Global Ecology Unit CREAF-CSIC-UAB, Barcelona 08193, Spain

ARTICLE INFO

Article history:
Received 16 February 2025
Received in revised form 11 September 2025
Accepted 12 September 2025
Available online 21 January 2026

Keywords:
Impervious surface
Spatial pattern
Driving mechanism
Border areas

ABSTRACT

Border areas between neighboring countries are crucial for the national and global success of sustainable development. These regions have witnessed rapid and widespread changes in land cover and use, especially the expansion of impervious surface areas (ISA). However, the global patterns and driving factors for this expansion are not well understood. We investigate ISA expansion in global borderlands by integrating high-frequency time-series satellite data, revealing that ISA has doubled between 1985 and 2020. The expansion is more pronounced in border areas with significant economic income disparities between countries, suggesting an overall attraction effect. Notably, 44 out of 310 borderlands (14%) accounted for 50% of ISA expansion over the past 36 years. Around one-third of global borderlands exhibit border-oriented development tendencies or border-prone characteristics. Our correlation and causation analyses indicate that population growth and topography are the primary drivers, with slight variations across different expansion modes. Understanding these border-prone characteristics and the underlying reasons for ISA expansion provides new empirical insights into urban sprawl, ecological environments, and sustainable development in border areas.
© 2026 The Authors. Published by Elsevier B.V. and Science China Press. This is an open access article under the CC BY license (http://creativecommons.org/licenses/by/4.0/).

1. Introduction

Impervious surface area (ISA) represents a major human disturbance to natural ecosystems and has increased significantly over recent decades [1–3]. Projections indicate that this trend will continue [4], with global urban land areas expected to be three times larger by 2030 than in 2000 [5,6]. This expansion is closely linked to several ecological and socio-economic consequences, including higher per capita urban greenhouse gas emissions, habitat fragmentation, biodiversity decline, inefficient resource use, and loss of farmland [7–10]. Furthermore, the continued growth of ISA was closely related to several Sustainable Development Goals (SDGs) [11], particularly SDG 11 (sustainable cities and communities) and SDG 15 (protecting terrestrial ecosystems). Despite its importance, our understanding of the extent, dynamic patterns, and potential mechanisms of ISA expansion, particularly in border areas, is limited. This limitation affects progress in the ability of border areas toward achieving SDGs by 2030.

A recent global study indicates that over one-sixth of the world's population and one-fifth of growth have occurred in border areas, contributing to 16% of land use changes [12]. Apart from agricultural-forest conversion, borderlands are experiencing profound and irreversible ISA expansion with varying degrees, or border-oriented development trend in near-border areas, such as cross-border twin cities, due to increased construction in various border towns, crossing ports, and economic cooperation zones between neighboring countries [13,14]. Existing global ISA-related analyses are mostly focused on administrative or watershed units [15–18], while ISA growth across border areas received less attention and remained sparsely, sporadically, and scatteringly investigated [19]. While this expansion provides opportunities for improved the well-being of border residents, it also exerts considerable pressure [20–22], particularly given that approximately one-third of the world's terrestrial biodiversity hotspots are located in border areas [23–25]. Notably, border areas differ fundamentally from inland areas because land policies, infrastructure networks, and ecological corridors must reconcile two (or more) sovereign decision systems that often have divergent priorities.

Globally, 60% of land use change is directly attributable to human activities, while the remaining 40% is driven by indirect factors such as climate change [26–28]. The expansion of ISA is influenced by a complex interplay of socio-economic factors (e.g., population growth, economic development, and policy systems)

* Corresponding authors.
E-mail addresses: fengzm@igsnrr.ac.cn (Z. Feng), wucy@igsnrr.ac.cn (C. Wu).

https://doi.org/10.1016/j.scib.2026.01.049
2095-9273/© 2026 The Authors. Published by Elsevier B.V. and Science China Press.
This is an open access article under the CC BY license (http://creativecommons.org/licenses/by/4.0/).

and natural environmental elements [20,29,30]. Meanwhile, topographical factors like slope and elevation also play an important role in ISA change in remote areas [31–33]. Additionally, a significant correlation exists between the expansion of ISA and a country's average income level [15]. Notably, as regional economic integration accelerates with cross-border activities and networks, neighboring countries are increasingly fostering connections in borderlands, significantly influencing ISA changes [34–36]. This institutional and socio-economic asymmetry makes borderlands a natural laboratory for understanding how contrasting national contexts co-shape impervious-surface dynamics. However, compared to analyses prioritizing hotspots and/or global-level mechanisms, cause-effects, and impact-responses of ISA growth across border areas still lack comprehensive and quantitative investigations, or are still in their initial stages [12]. Although some studies have quantified the potential correlated factors of border ISA expansion, they have mainly focused on only border cities or single cross-border economic cooperation zone [13,19]. Therefore, investigating border-ISA changes is of profound significance for enhancing cross-border land planning, addressing unbalanced regional development, optimizing spatial resource allocation, and advancing collaborative ecological governance over the borderlands.

Here, we quantitatively analyzed the spatio-temporal distributions, evolution patterns, and underlying mechanisms of ISA in global border areas from 1985 to 2020. Our analysis addressed the following questions: (1) What is the scale of ISA expansion in border areas, and how is it related to differences in income levels between countries? (2) What are the spatial patterns of ISA expansion in border areas over the past 36 years? (3) What factors have driven the expansion of ISA in borderlands globally? This study aims to provide a more holistic understanding of the dynamics shaping ISA expansion in border areas, thereby contributing to the achievement of sustainable border development under the umbrella of the SDGs. Additionally, our study provides data support and methodological reference for exploring the border effect.

2. Study area

Border areas specifically refer to regions along the boundaries of neighboring countries, which are closely located across an international border. In international border studies and national border management, the width of borderlands is defined differently across various contexts. For instance, some studies designate borderlands as 2-km wide (e.g., between Democratic People's Republic of Korea and Republic of Korea [37]), over 5-km (e.g., between Russia and Finland [38]), 20–30 km (e.g., in China [39]), 30–50 km (e.g., in the European Union [40]), or 60-km wide (e.g., in the United States [41]) along the national boundary. In order to create global uniformity and following the perspective of the U.S.-Mexico border study [41], we defined border areas as buffer zones that extend 60 km on both sides of the national boundary (Table S1 online). However, the analysis exclusively on the border region of 60 km does not go far enough, since dynamics are very different across the globe. Therefore, to retain spatial detail, we also compute statistics for each 1-km ring between 1 and 60 km. Additionally, we further define the 0–30 km buffer zone as the near-border areas (Table S2 online). In this study, we initially identified the border areas of 313 pairs of countries across five continents: Asia, Africa, Europe, North America, and South America [42]. Statistical data indicate that global border areas cover approximately 1/12 of the Earth's land surface. Notably, out of these 313 pairs of border countries, 310 have monitored ISA and their changes, while the Libya-Niger (LY-NE), Libya-Sudan (LY-SD), and Libya-Chad (LY-TD) pairs in borderlands (60-km buffer zone) have no construction land. Therefore, our analysis focuses mainly on these 310 pairs of border areas (Fig. 1).

3. Materials and methods

3.1. Data sources

This study utilizes multi-source data, including global land use data and covariates from 1985 to 2020, as well as the World Bank Group's country classification by income level for 2020, to comprehensively reveal the dynamic processes and national differences of ISA expansion in global border areas as well as their potential mechanisms underlying (Table S3 online). Notably, discrepancies among widely used land use datasets among 30-m GISD30 [3], 30-m GAIA [1], 30-m GISA [2], and 300-m ESA CCI [43] underscore the complexity and uncertainty of accurately measuring ISA. For example, in 2015, GISD30 reported the largest border ISA of 1.75×10^5 km^2, which was substantially larger than GAIA (0.88×10^5 km^2), GISA (1.02×10^5 km^2), and ESA CCI (1.36×10^5 km^2). To address these discrepancies, we validated the results using an independent set of 10,000 randomly selected points, confirming GISD30's superior performance in border regions (Fig. S1 online). The overall accuracy and kappa coefficient of the 30-m GISD30 datasets are 87.3% and 0.83, which can meet the data requirements of this study.

About the driving factors of ISA expansion in the borderlands globally, we categorized them into three groups, including socio-economic factors, physical constraints, and natural environmental factors (Table S4 online). Specifically, we used population, gross domestic product (GDP), nighttime lighting (NTL), and road networks as indicators of socio-economic development; digital elevation model (DEM), slope, and relief degree of land surface (RDLS) as physical constraints; and normalized difference vegetation index (NDVI), precipitation, annual average temperature, annual maximum temperature, and annual minimum temperature as natural environmental indicators (see Supplementary Data for detailed description). To ensure spatial consistency, all driver layers were harmonized to a 1 km × 1 km grid before analysis. Additionally, to briefly assess the potential impact of ISA expansion on biodiversity, we selected an independent dataset of 36 established biodiversity hotspots [44] and examined their spatial overlap with the ISA expansion in the borderlands globally.

3.2. Gaussian function fitting-derived border ISA mode

To analyze global border ISA expansion patterns, we applied Gaussian function fitting to categorize them into five types: off-bordering (Fig. S2 online), border-prone (Fig. S3 online), U-shaped (Fig. S4 online), ∩-shaped (Fig. S5 online), and random mode (Fig. S6 online). The Gaussian function [45] fitting helps identify trends in ISA growth by fitting distance (0–60 km from the border) and expansion data. The Gaussian curve's center (parameter b) determines the classification: border-proximal, border-distal, U-shaped, or ∩-shaped. The analytic process overview of the Gaussian function for ISA expansion patterns is shown in Fig. S7 (online). To assess the statistical significance of the fitted curves, we calculated the P-value for each curve. A P-value less than 0.05 indicates that the observed relationship is statistically significant, suggesting that the fitted Gaussian model effectively represents the ISA expansion pattern. In cases where the Gaussian fit was not statistically significant, we employed a fifth-degree polynomial fit as an alternative. For both methods, we examined curve trends and used parameter values to classify expansion types, ensuring comprehensive coverage of different ISA dynamics in 310 global border areas. These fitting methods enabled systematic identification of ISA patterns and offered valuable insights into borderland development dynamics, as demonstrated in related land use studies. However, potential biases and assumptions in

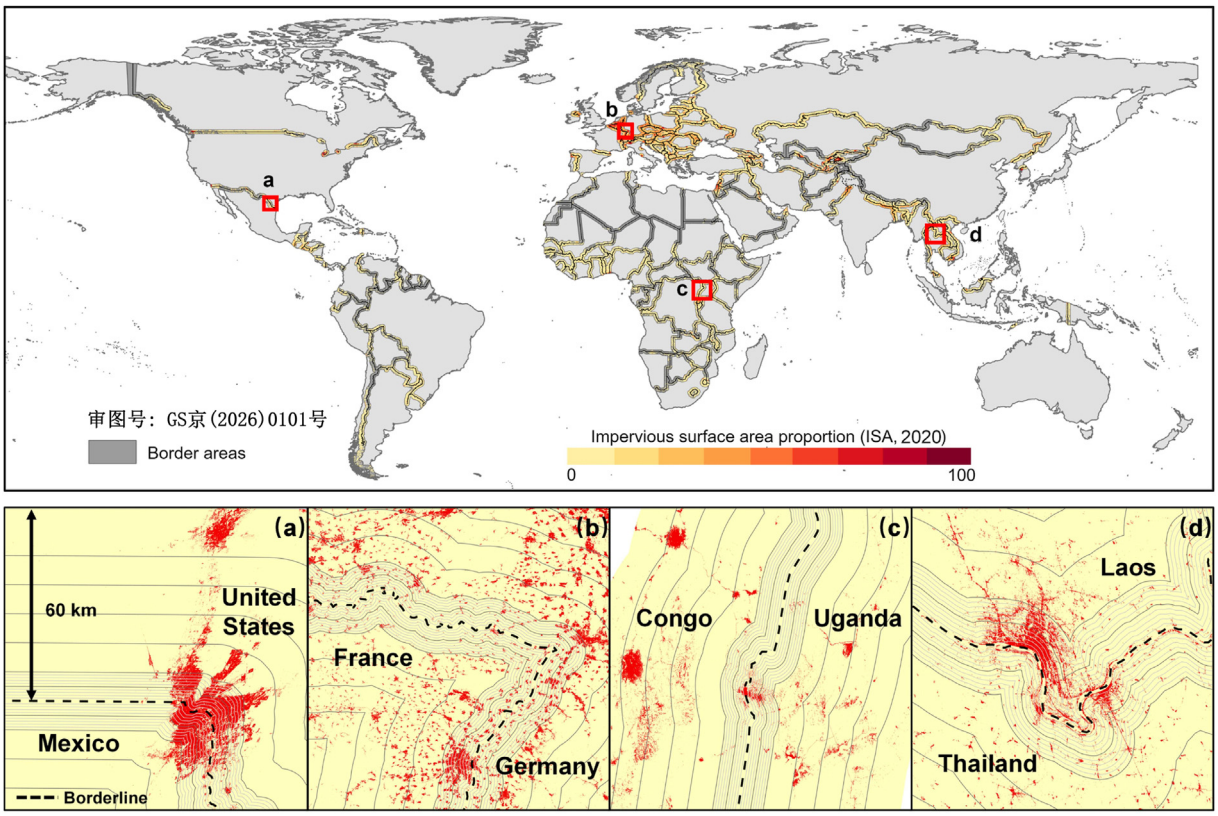

Fig. 1. Spatial distribution of ISA proportion in global borderlands as of 2020 based on the 30-m GISD30 dataset. This comprehensive visualization of ISA within 10 km × 10 km grid cells encompasses the entirety of the world's 60-km border zones. The subpanels (a–d) represent detailed insets of selected regions like borders of the United States-Mexico (a), France-Germany (b), Cong-Uganda (c), Laos-Thailand (d), highlighting specific areas of notable ISA along international boundaries.

curve interpretation could affect classification accuracy, highlighting the need for refining these methods or integrating additional data in future research.

3.3. Driving mechanism analysis

In the driving mechanism analysis section, we employed two complementary approaches to examine the relationship between ISA expansion and driving factors. First, we used Geographic Convergent Cross Mapping (GCCM) to explore potential causal relationships between ISA expansion and driving factors. GCCM can identify whether changes in driving factors can predict ISA expansion over time, based on the spatial-temporal dynamics. Second, we applied Shapley Additive Explanations (SHAP) values derived from the XGBoost model to quantify the relative importance and interactions of the driving factors, providing a deeper understanding of how each factor contributes to ISA expansion. While GCCM identifies causal links, SHAP values offer insight into the predictive power and interaction effects of these factors within the XGBoost framework. Together, these approaches allowed for a more comprehensive analysis of the underlying mechanisms driving ISA expansion. The detailed description of the analysis modelling framework, of independent variables and dependent variables can be found in the Supplementary Methods.

Causal inference with GCCM model. In general, the drivers of ISA expansion in the borderlands globally are complex. To analyze the causal relationships between spatial units, we employed the GCCM method, aiming to explore the causal relationships between ISA expansion and multiple potential driving factors. The GCCM model, based on dynamic systems theory and generalized embedding theory [46,47], tests whether the spatial distribution of one variable can accurately predict the spatial distribution of another, revealing potential causal relationships. The strength of these causal relationships does not always directly translate into their contributions. Given the strip-shaped border areas and scattered ISA expansion, we modified the traditional GCCM method to better suit these characteristics.

We defined ISA expansion as the target variable, labeling ISA existing before 1985 as original (0), and those expanded between 1985 and 2020 as 1. Twelve potential driving factors, including socio-economic factors (e.g., GDP), natural environmental factors (e.g., NDVI), and physical constraints (e.g., RDLS), were identified. To ensure GCCM accuracy, we applied ordinary least squares regression to eliminate primary linear trends in these variables [48]. For each variable, we predicted based on the nearest neighbors identified from another variable, utilizing the nearest neighbor algorithm to select spatial neighbors, considering spatial dependency. Data were reconstructed according to selected neighbors and embedding dimensions to capture spatial lag effects, particularly considering the strip-shaped characteristics of border areas and scattered distribution of ISA expansion.

XGBoost model. Tree-based machine learning models are highly popular nonlinear models used in geoscientific dynamic prediction and attribution analysis [49]. They often outperform neural networks in accuracy and exceed standard deep learning models on tabular datasets [50]. Extreme Gradient Boosting (XGBoost) is an ensemble learning algorithm built from iterative decision tree models and widely applied in classification and regression tasks [51].

Here, we employed the nonlinear XGBoost algorithm to model the ISA expansion in the borderlands globally driven by 12 different factors, including socioeconomic factors, natural environmen-

tal factors, and physical constraints. ISA existing before 1985 were defined as the original ISA (labeled as 0), while grid points that expanded between 1985 and 2020 were labeled as 1. To prevent overfitting, we utilized correlation analysis (r) and the Variance Inflation Factor (VIF) [52] to eliminate variables with low predictive ability, ensuring only the most relevant features were included in the model (Fig. S8 online). The XGBoost component of the GCCM framework was implemented in Python and first subjected to ten - fold cross validation across all 310 border pairs, returning mean test fold scores of R^2 = 0.73 and ROC AUC = 0.80, which indicates strong in sample generalization. To further assess spatial transferability, we applied a leave one out protocol in which border pairs from Africa, Asia, Europe, and the combined Americas were used for training while the held out continent served as the validation set (Oceania was excluded because our 60 km buffers contain no within continent land borders there); this yielded a mean R^2 = 0. 70 ± 0.04 and ROC AUC = 0.78 ± 0.05. The full validation curves and confidence intervals are shown in Fig. S9 (online).

Explainable predictions of SHAP model. The SHAP model is derived from the Shapley value concept in game theory [53] and is considered an improvement over the Local Interpretable Model-agnostic Explanations (LIME) approach. The XGBoost-SHAP framework has been successfully applied to local explanations in fields such as residential buildings and socio-economic sciences [54]. This method directly monitors the impact of individual features (e.g., population, GDP, and RDLS) on model loss, specifically the differences between the predicted values and the expected values of global ISA expansion. SHAP calculates the average marginal contribution of each feature across all possible combinations, assigning importance values that reflect local interaction effects [50]. For a specific input sample x with M features, the Shapley additive mechanism can be represented by decomposing an individual prediction into feature contributions [55]. The SHAP method can also be used for global explanations [56]. In this study, we applied the SHAP method to detect factor effects (SHAP values) and main effects (SHAP main values, without interactions with other input variables). Using a set of tools within the SHAP framework, we can more clearly and easily interpret the impact mechanisms of socioeconomic factors, natural environmental factors, and physical constraints on ISA expansion. The patterns of feature importance and SHAP values remained consistent.

4. Results

4.1. One-seventh of border areas contributed to half of the ISA increase

Since the 1980s, border areas experienced a doubling of ISA (from 1.21×10^5 km^2 in 1985 to 2.23×10^5 km^2 in 2020) expansion of ISA (Fig. 2 and Table S1 online). Fig. 2a shows the spatial dynamics and variations of ISA in borderlands globally from 1985 to 2020. ISA with high growth rates were mainly concentrated in North American (e.g., US-CA), European (e.g., NL-BE), and Asian (e.g., RU-CN) borders. Compared with other continents, areas with lower growth rates were primarily found in Africa's and South America's border areas in the last 36-years. Importantly, the distribution and percentage increase of ISA in the border areas displayed a significant north-south difference, with areas north of 30°N primarily characterized by high values (Fig. 2a). By contrast, areas south of 30°N exhibited a notable increase in ISA over time. The growth of ISA in border areas accounted for about one-sixth of the total global level over the past 36 years, with an average annual growth rate of 2.7%. Notably, around the year 2000, the growth rate of ISA accelerated significantly, increasing from an average of 7.1% (±1.1%) to 13.9% (±1.1%).

As it showed above, the average area of border ISA and the related area proportions varied dramatically at the national level (Fig. 2c and Table S1 online). The results indicated that one-seventh (44 pairs) of the 310 global border country pairs contributed to half of the ISA increase in the borderlands globally between 1985 and 2020. We also found that the top five border pairs (1.6%) accounted for 10% of the global increase (Fig. 2c). Among them, the US-CA border alone added 3193 km^2 (2.9%) of new-added ISA, with the remaining top pairs in Asia, including the KH-VN border in Southeast Asia (2.4%), KG-UZ and TJ-UZ borders in Central Asia (both 2%), and the BD-IN border in South Asia (1.96%).

We further used the World Bank Group's country classification by income level (Table S3 online) to reveal the differential impacts of national economic scale on the expansion of ISA along borders (Fig. 2d). The results indicated that the economic scale of different countries significantly affected ISA expansion along borders, with high-income countries playing a dominant role in the overall growth of ISA in border areas, such as the US-CA border. Specifically, the median growth area for borders between high-income and low-income countries (H-L) was the highest among all types at 462.6 km^2, indicating an attraction effect. Subsequently, the median growth areas for borders between high-income and high-income countries (H-H) and between high-income and upper middle-income countries (H-UM) were 388.9 and 285.4 km^2, respectively. Interestingly, despite the predominance of growth driven by high-income countries, borders between lower middle-income countries (LM-LM) also showed significant growth, with a median growth area of 243.8 km^2.

4.2. One-third of borders exhibit border-prone characteristics of ISA in the near-border areas

Using a Gaussian function-fitting model-derived distance from area changes of national boundary-based estimates as a baseline, we determined five spatial patterns of ISA expansion in border areas (see Fig. 3, Methods, and Supplementary Methods): off-bordering, border-prone, U-shaped, ∩-shaped, and random mode. Fig. 3a shows the spatial distribution of these five patterns, along with their corresponding expansion area per km within a 60-km buffer zone of borders over a 36-year period. Among the 310 pairs of national borders, from a numerical perspective, the predominant mode of ISA expansion was off-bordering characteristics or mode 1 (Fig. 3b), comprising about 31% (96 pairs, Fig. S2 online). In these cases, development occurred primarily away from the border. For example, the Cambodia-Vietnam border followed this pattern, with significant ISA expansion observed away from the border within the 60-km buffer zone.

Border-prone characteristics, or mode 2 (Fig. 3b), represented 19% of the cases (60 pairs, Fig. S3 online), with construction and development increasingly concentrated near the border. The United States-Mexico border exemplifies this pattern, highlighting the importance of effectively managing border ISA expansion. The U-shaped characteristic or mode 3 (Fig. 3b) accounted for 6% (18 pairs, and Fig. S4 online), while the ∩-shaped characteristic or mode 4 (Fig. 3b) accounted for 17% (55 pairs, and Fig. S5 online). These patterns respectively represented alternating expansion near and away from the border as well as regular fluctuations. The Algeria-Morocco border and the Kazakhstan-China border clearly demonstrated U-shaped and ∩-shaped modes, respectively. The remaining 27% (84 pairs, and Fig. S6 online) showed random characteristics or mode 5 (Fig. 3b), indicating insignificant changes or disordered distribution of ISA expansion.

From 1985 to 2020, the total expansion area of impervious surfaces in global border areas reached 1.02×10^5 km^2. Among these, off-bordering characteristics dominated, accounting for 34% (3.5×10^4 km^2) of the total, followed by random with 2.56×10^4 km^2 (25%), border-prone with 2.1×10^4 km^2 (21%), ∩-shaped with 1.48×10^4 km^2 (14%), and U-shaped with

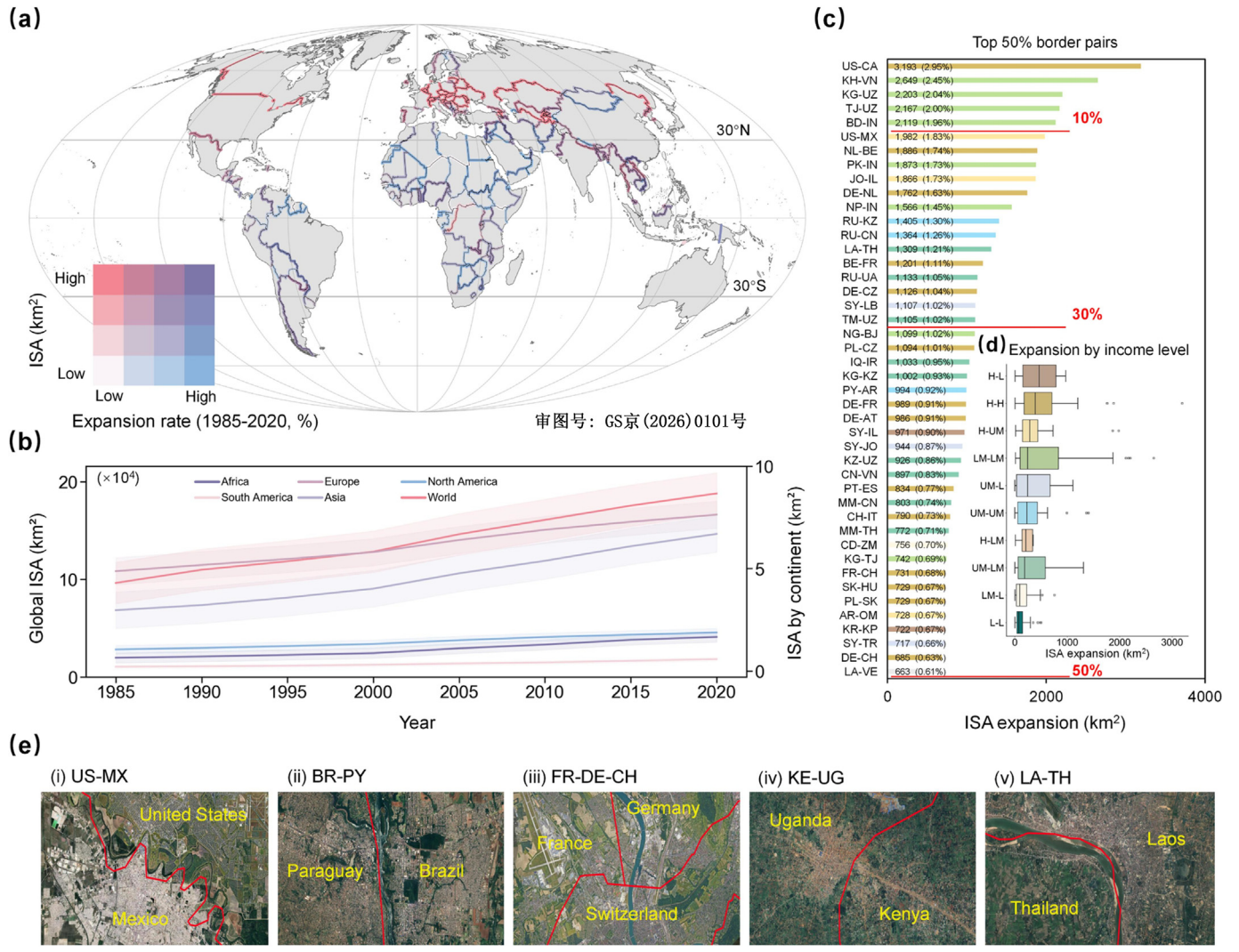

Fig. 2. Spatial patterns and trends in ISA expansion at borderlands globally from 1985 to 2020. (a) ISA distribution and expansion rates at global borders in 2020. Color-coded by area and expansion rate: purple (high area, high rate), blue (low area, high rate), pink (high area, low rate). (b) ISA expansion trends across global and continental borders (Africa, North America, Asia, Europe, South America). (c) Top 44 border pairs by ISA area and proportion, ranked from highest to lowest. Bar chart displays numbers and percentages; cumulative expansion marked at 10%, 30%, and 50%. (d) ISA expansion distribution by income level pairs (H: high income; L: low income; UM: upper middle income; LM: lower middle income). (e) Aerial and remote-sensing views of ISA homogeneity and heterogeneity in selected global borderlands (e.g., US-MX, BR-PY). Red lines indicate national boundaries; ISO country codes are provided in Table S1 (online).

0.65×10^4 km^2 (6%). We also found that the current area proportions of various expansion patterns were consistent with the proportions of their expansion areas. Notably, in the near-border areas (0–30 km buffer zone), border-prone characteristics of ISA were particularly prominent, reaching 2.56×10^4 km^2 (31%) and 1.31×10^4 km^2 (32%) for current and expansion areas, respectively (Table S2 online). This indicates a clear border-prone trend in ISA near-border areas. Similarly, off-bordering and random modes also exhibited expansion trends, with incremental areas of 0.97×10^4 km^2 (24%) and 0.98×10^4 km^2 (24%), and current areas of 2.07×10^4 km^2 (25%) and 2.11×10^4 km^2 (25%), respectively. The distributions of ∩-shaped and U-shaped features in near-border areas matched the broader borderlands, with expansion of 0.52×10^4 km^2 (13%) and 0.30×10^4 km^2 (7%), respectively.

4.3. Population growth-induced ISA expansion regulated by topography

Through Granger causality cross-mapping (GCCM) analysis, we observed a broad causal relationship between ISA expansion (including the five patterns: off-bordering, border-prone, U-shaped, ∩-shaped, and random) and socio-economic, physical constraint, and natural environmental factors (P = 0.00) (Fig. 4a and Figs. S10–S14 online). Socio-economic factors had the greatest impact on ISA expansion, particularly population growth (ρ = 0.94), GDP (ρ = 0.82), and road density (ρ = 0.79). In fact, both population and topographic features slope have a significant influence on ISA expansion, particularly in the early stages of border development. Among physical constraint factors, slope (ρ = 0.94) and elevation (ρ = 0.71) significantly influenced ISA expansion, while temperature-related natural environmental factors also showed notable effects. Using SHapley Additive exPlanations (SHAP) values from the XGBoost model, we further quantified the roles of these factors in border ISA expansion (Fig. 4b–d and Fig. S9 online).

Specifically, population growth had the highest SHAP value (mean |SHAP| = 0.39), indicating a strong impact on border ISA expansion, particularly in low-growth areas. Slope (mean |SHAP| = 0.28) and elevation (mean |SHAP| = 0.16) also played noteworthy roles in physical factors, reflecting the impact of ter-

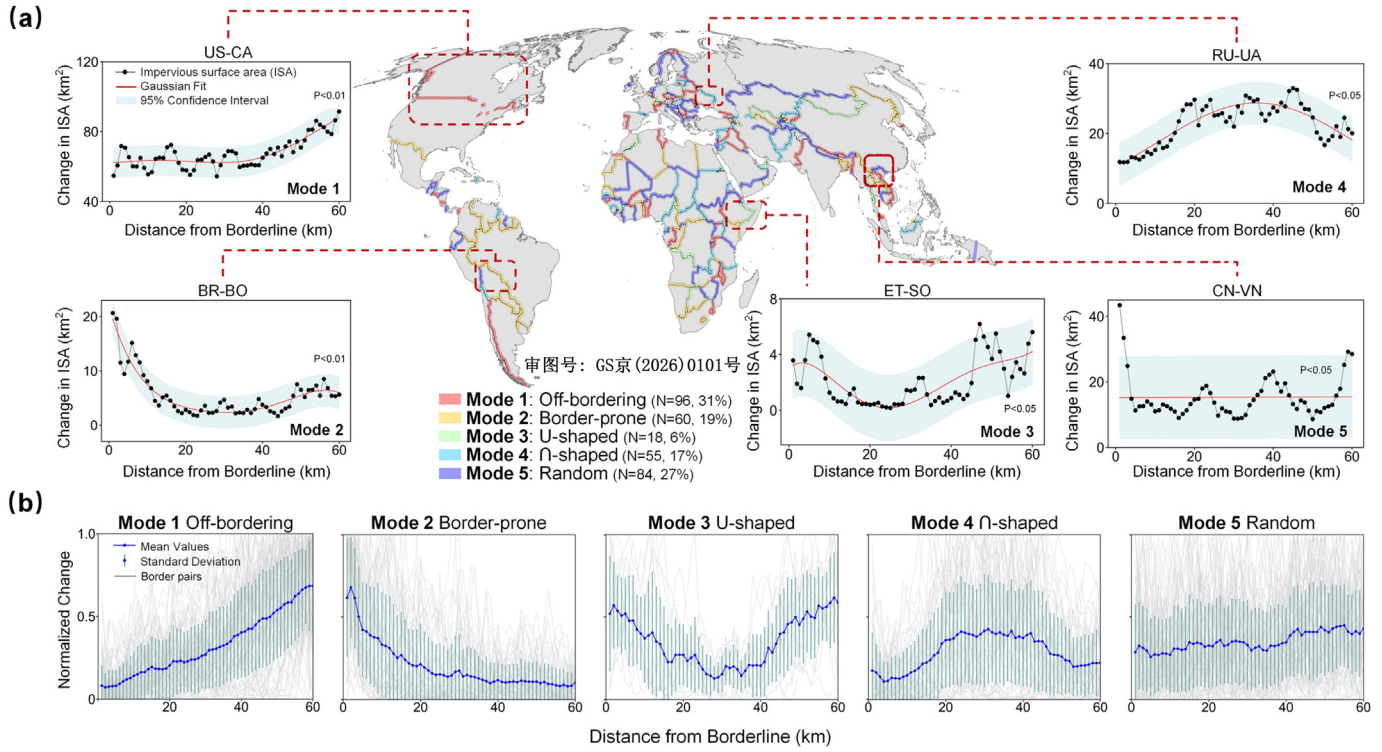

Fig. 3. The five expansion patterns of ISA in global border areas. (a) Different colors represent the spatial distribution of different expansion characteristics, obtained from Gaussian function: Mode 1 (31%, red, off-bordering characteristics), Mode 2 (19%, yellow, border-prone characteristics), Mode 3 (6%, green, U-shaped characteristics), Mode 4 (17%, blue, ∩-shaped characteristics), and Mode 5 (27%, purple, random characteristics) (see Supplementary Method for the model details). Insets present global-to-national scale examples of the five models, depicting trends in ISA change with distance from the borderline. Black dots represent observed values, dashed lines represent Gaussian fit curves, and shaded areas show the 95% confidence intervals. Examples include the US-CA (United States-Canada, Mode 1), BR-BO (Brazil-Bolivia, Mode 2), ET-SO (Ethiopia-Somalia, Mode 3), RU-UA (Russia-Ukraine, Mode 4), CN-VN (China-Vietnam, Mode 5) borders. (b) Detailed display of the overall expansion trends of 310 datasets, with each subplot corresponding to one mode (Figs. S2–S6 online). The horizontal axis, vertical axis, blue lines, green area, and gray lines represent the distance from the borderline (in km), expansion proportion, average trend, data variance, and changes per km of ISA in different border pairs.

rain conditions on ISA expansion. Overall, population growth-induced ISA expansion in global border areas has been regulated by topography over the past 36 years. Additionally, annual maximum temperature (mean |SHAP| = 0.27) was significant among natural environmental factors, especially in regions with well-developed infrastructure or favorable climate conditions. SHAP results also revealed variations in the roles of road density, nighttime lights, and other natural factors, such as precipitation and vegetation cover, across different regions. Although the average SHAP values for these factors were lower, they could still significantly impact ISA expansion under specific regional conditions.

Compared to the entire global borderlands, the five ISA expansion patterns—off-bordering characteristics (Fig. 5a), border-prone characteristics (Fig. 5b), U-shaped characteristics (Fig. 5c), ∩-shaped characteristics (Fig. 5d), and random characteristics (Fig. 5e)—showed differences in driving factors and causality, primarily influenced by GDP, road density, RDLS, and population growth. Within these five patterns, GDP changes (mean |SHAP| = 0.47) were the major driving factor in the off-bordering mode, followed by RDLS and population growth. In the ∩-shaped and random modes, GDP variation was the dominant factor (mean |SHAP| of 0.5 and 0.46), with significant contributions from population growth. For physical constraint factors, ∩-shaped characteristics were predominantly influenced by elevation (mean |SHAP| = 0.41), while random characteristics were influenced by RDLS. For border-prone characteristics, RDLS and socio-economic factors of GDP and population growth were the dominant factors. Notably, the U-shaped modes showed similarities with overall global trends, primarily driven by population expansion, followed by NDVI and RDLS. In summary, socio-economic factors (namely, population and GDP) and physical constraints (e.g., RDLS) jointly regulated global border ISA expansion, showing broad regional variations.

5. Discussion

5.1. Driving mechanisms of ISA expansion in border areas

Our findings demonstrate that population-induced ISA expansion is accelerated by border-prone expansion regulated by topography over border areas globally, with five different expansion modes showing slight variations. Since 2001, the population in borderlands globally has increased by 41%, with an additional 1.4 billion people, directly leading to infrastructure development and an ISA boom [42,57,58]. This highlights the importance of understanding ISA in global border areas within the context of significant population growth concerning sustainable development and border security [59]. Additionally, topographical factors, such as mountains and rivers, significantly influence ISA expansion by limiting or directing its spread. These natural barriers interact with the population [13], complicating border ISA development. Notably, when examining the five expansion patterns, factors like GDP and RDLS emerge as more significant (Fig. 5). For example, in off-bordering and random patterns, ISA is often dominated by GDP changes, underscoring the impact of economic activities and development levels. Obviously, economic cooperation or competition and cross-border development among neighboring countries often lead to increased infrastructure and commerce, driving border ISA expansion [14,19,60]. While we adopted a more advanced

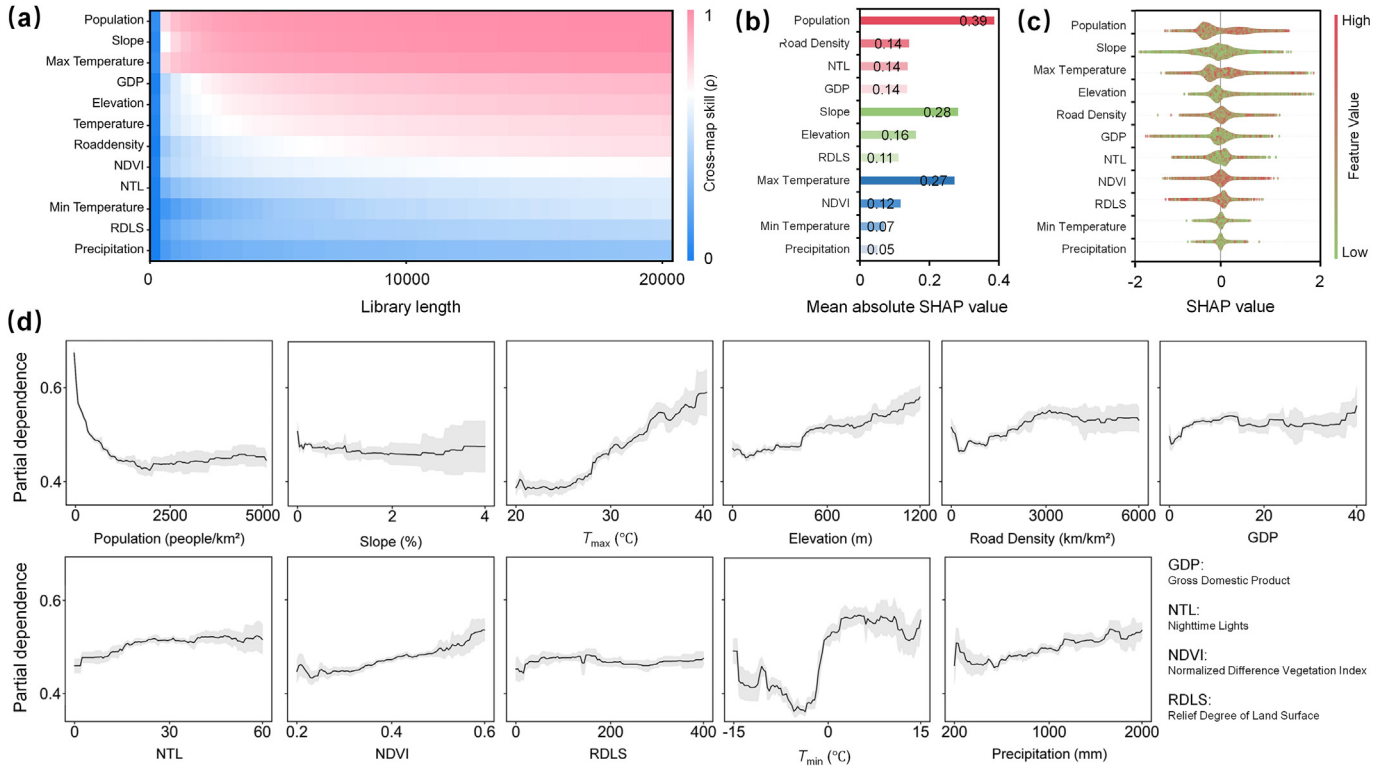

Fig. 4. Importance of different driving factors for the expansion of ISA in global border areas. (a) The cross-mapping prediction output for ISA expansion in borderlands and various potential driving factors analyzed with the maximum library size. A higher *P*-value for Y xmap X represents a stronger causal relationship from the driving factor (X) to ISA expansion (Y). (b) The mean absolute SHAP values for each predictor, reflecting their importance in the XGBoost model (see Supplementary Method for the model details). (c) SHAP value distributions for each predictor, with colors indicating feature values (red for high values and green for low values). Distribution plots illustrate the positive and negative impacts of different predictors on the model output. (d) Line charts in various colors show the effect of changes in each predictor on the model's prediction results, with each subpanel representing one predictor. The red line indicates the average trend, and the gray area represents data variance.

GCCM and XGBoost models that provide valuable insights into causality and drivers [46], they often overlook the complex interplay of these factors in border areas. Thus, impact-responses and contributions of geopolitical economic relations on border ISA should be incorporated into future assessments for their accuracy and explanatory power.

5.2. The impact of border ISA expansion

Border areas, which are key to the national and global success of sustainable development [11]. While the socio-economic benefits of ISA expansion in border areas are evident, and have far-reaching eco-environmental and political impacts, which demand urgent attention to address multiple global SDGs [23]. For instance, the increase in infrastructure construction (e.g., cross-border corridors and economic cooperation zones) has greatly improved the livelihoods and traffic accessibility of cross-border dwellers [61]. Yet replacing carbon-rich ecosystems and/or vegetated land with ISA leads to local and trans-national eco-environmental consequences and controversies, even broader international challenges, like cross-border carbon emissions as well as transboundary water and air pollution [62–64]. In addition, large-scale border ISA expansion with cross-border and/or borderlands population movement and trade may further trigger potential consequences and regarding national relations, border security, infectious diseases, as well as smuggling and crime [12]. Importantly, there is spatial overlap between border areas and one-third of terrestrial biodiversity globally (Fig. S15 and Table S5 online). We believe further in-depth analyses of the cause-effect and impact-response of ISA expansion on biodiversity are needed. Regions like the Atlantic Forests (92%), Mediterranean Basin (22%), Caribbean Islands (13%), and West African Guinea forests (21%) have seen severe habitat fragmentation, restricting species migration and reproduction [44,61]. Therefore, biodiversity conservation in border areas requires transboundary joint efforts [6,65]. Under the SDGs, establishing cross-border cooperation mechanisms to enhance coordination among neighboring countries in biodiversity conservation through multi-dimensional protection policies is essential [66,67].

5.3. Comparison of ISA expansion across different income levels

We also found that ISA expansion in border areas varies significantly across different income levels. For example, border areas between high-income and low-income countries (H-L) experience rapid ISA growth, driven by the migration of labor and businesses seeking better economic opportunities in high-income regions [68], which accelerates urbanization and infrastructure development [69]. This phenomenon may be related to the attraction effect that high-income countries exert on low-income ones [70,71]. Additionally, borders between high-income countries (H-H) also exhibit considerable ISA expansion due to advanced infrastructure integration and strong economic ties [72,73]. Generally, high-income countries have developed markets, relatively high labor mobility, mature agglomeration economies, and high-quality urban infrastructure and services. In contrast, lower-middle-income countries (LM-LM) demonstrate substantial ISA expansion through cooperative development efforts [74]. These countries often collaborate on joint infrastructure projects and regional development plans, enhancing their collective economic strength and competitiveness [75]. These findings suggest the need for tailored sustainable development and border-city or town planning strategies that account for the specific socio-economic contexts

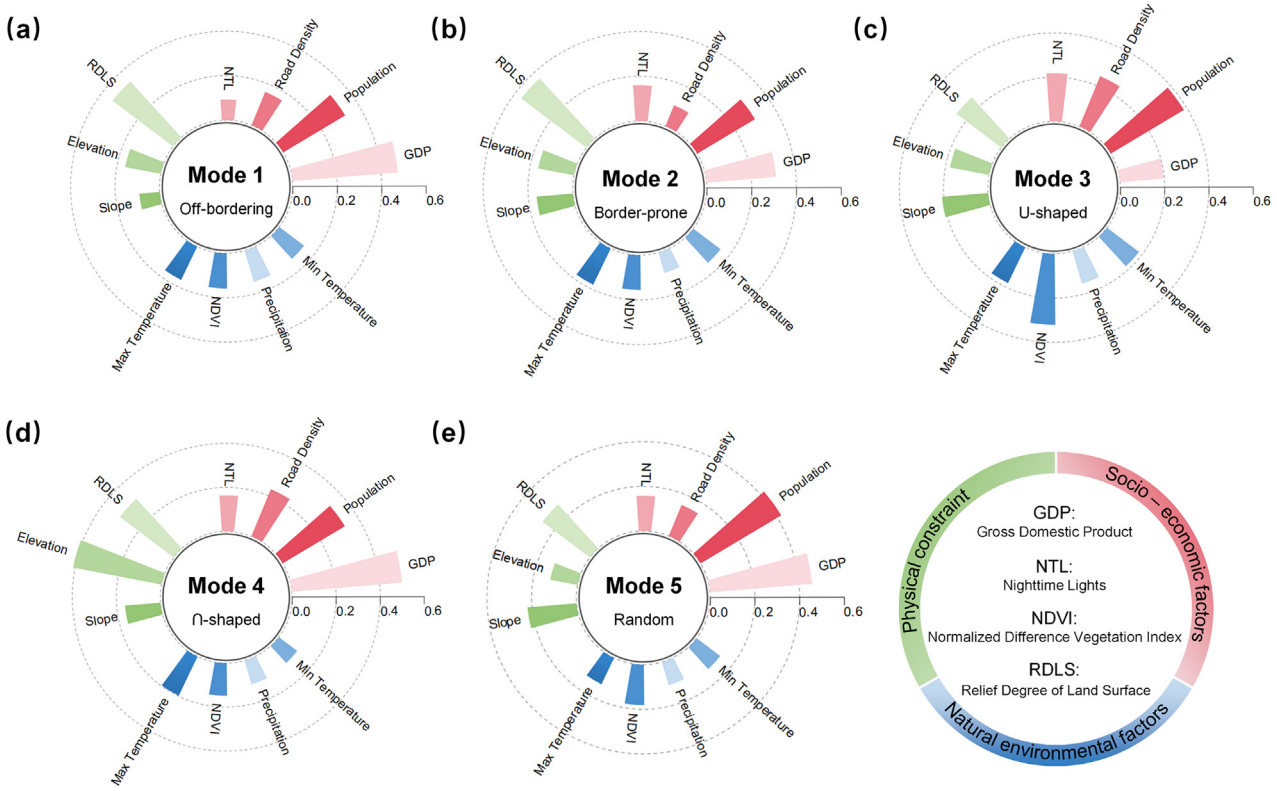

Fig. 5. Underlying mechanisms for the five patterns of ISA in global border areas. (a–e) Results showing the importance of different predictors in XGBoost model used to predict off-bordering characteristics (a), border-prone characteristics (b), U-shaped characteristics (c), ∩-shaped characteristics (d), and random characteristics (e), respectively. In (a–e), each panel lists predictors ranked by their mean absolute SHAP values, indicating their relative importance in the models.

of each national border [76]. This cooperative approach contrasts with the more competitive dynamics observed between upper middle-income countries (UM-UM), where ISA expansion is relatively slower. Our findings highlight that a better understanding of border-prone characteristics of ISA expansion across different income levels underscores the importance of sustainable development strategies tailored to local conditions, providing essential knowledge and insights for implementing SDGs holistically.

5.4. Implications and outlook

We contribute to enriching this area of knowledge by integrating high-frequency time-series satellite data and covariates to first quantify the trends, patterns, and mechanisms of ISA expansion in global border areas. Our findings support the idea that geo-economic cooperation among neighboring countries enhances border ISA expansion [19,77] through regional integration, cross-border infrastructure policies, and migration [78–80]. In particular, border ports serve as key hubs for trade and migration, driving concentrated infrastructure growth [81–83], and are critical areas for ISA expansion [84]. We found that crossing ports and their adjacent areas accounted for 59% of border ISA in 2020 (Fig. 6). As the tip of the iceberg of frontier development, the border-prone characteristics of ISA growth not only mirror the evolving dynamics of international exchange and cross-border activities [85] but also represent a complex process shaped by various factors, such as geopolitical economic relations between neighboring countries [5,13,14]. We appeal that urgent priorities may be to launch global round tables or supranational initiatives among neighboring countries, local governments, nongovernmental organizations, and scientists under the umbrella of SDG, like the Global Border Observation for ISA (GBW_ISA), which might be initiated to focus on border development, including land use, biodiversity, and thematic surveys. Besides, spatially accurate and temporally dense or long-time series information for the ISA including the intensity of urbanization, and other typical land use (e.g., cropland) across borderlands and its key regions (e.g., border ports) should be tailored in the future, to meet the data demands necessary for sustainable border development assessment.

Although this study provides valuable insights into the expansion of ISA in global border regions, several limitations should be carefully considered. The datasets used in the study, exhibit discrepancies in spatial resolution and classification methods, which may lead to biases in the ISA expansion trends in regions with complex topography or sparse data. Additionally, the 60-km buffer zone definition may not be applicable to all border regions, particularly in smaller countries or areas with different ecological characteristics. To address this, we conducted a 1–60 km incremental buffer analysis, which showed that the near-border area (0–30 km) exhibited a more prominent border-prone expansion pattern. Future research could determine the most sensitive buffer distance for different regions through multi-scale analysis. Moreover, the GCCM and XGBoost models rely on specific assumptions that do not fully capture the complex dynamics of other factors [46], like geopolitical relationships, which may affect the accuracy of the ranking of driving factors. We have mitigated some of the uncertainty through multi-source data fusion, cross-validation, and supplementary analyses. Future studies will use high-resolution data (such as 10-meter Sentinel-2 imagery) and the GLOBIO model [86], along with species-level data (e.g., IUCN Red List) [87], to assess the specific impacts of ISA expansion on cross-border biodiversity (e.g., Mean Species Abundance), thus enhancing the representativeness of the results and the comprehensiveness of ecological impacts.

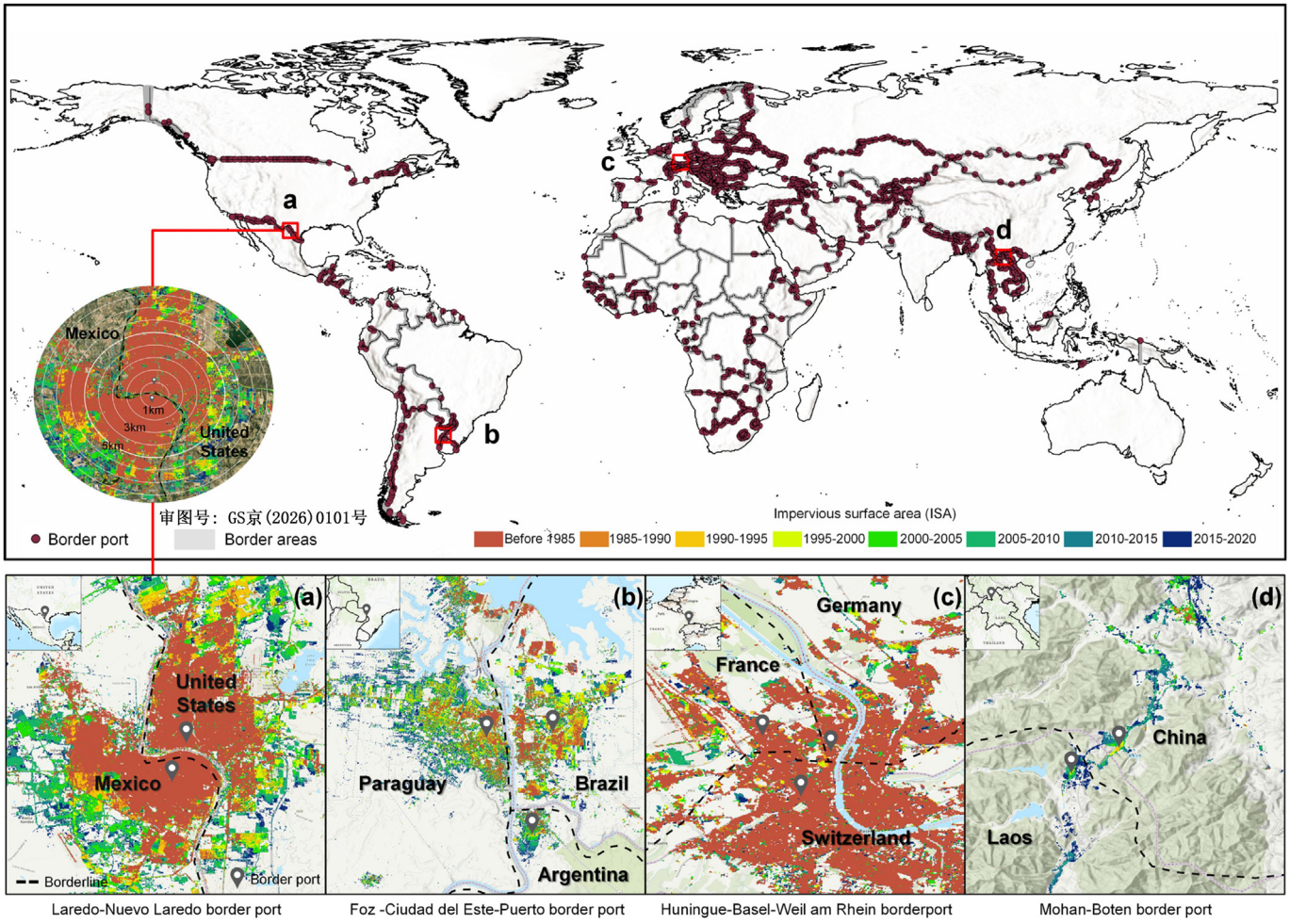

Fig. 6. The global distribution of border ports and delineates the expansion of ISA during different periods from 1985 to 2020. Border ports are represented by purple dots, border areas by grey lines, and the expansion of ISA over different periods is indicated by various colors, with each color corresponding to a five-year interval. (a–d) Detailed views of four typical border ports, including the Laredo-Nuevo Laredo border port between the United States and Mexico (a), the Foz-Ciudad del Este-Puerto border port (b), the Huningue-Basel-Weil am Rhein border port among Switzerland, France, and Germany (c), and the Mohan-Boten border port between China and Laos (d), respectively.

Conflict of interest

The authors declare that they have no conflict of interest.

Acknowledgments

This work was supported by the National Natural Science Foundation of China (42130508, 42125101, and 42371280) and the Programme of Kezhen-Bingwei Excellent Young Scientists of the Institute of Geographic Sciences and Natural Resources Research, Chinese Academy of Sciences (2022RC002). We thank all anonymous reviewers for their helpful remarks.

Author contributions

Chiwei Xiao proposed the original idea. Chiwei Xiao, Zhiming Feng, and Chaoyang Wu designed the research. Zilong Yue and Yi Wang performed the data analysis. Chiwei Xiao and Zilong Yue wrote the first draft of the paper. Chiwei Xiao edited and revised the manuscript in consultation with Chaoyang Wu and Zhiming Feng. Josep Peñuelas and Chaoyang Wu substantially revised the manuscript with intensive suggestions. All authors critically reviewed the manuscript and approved the final manuscript.

Data availability

All the data used in this study are available online via the following links: GISD30, https://zenodo.org/records/5220816; ESA CCI, https://www.esa-landcover-cci.org/; GISA, https://zenodo.org/record/5136330; GAIA, https://data-starcloud.pcl.ac.cn/zh/resource/13; Climate, https://chelsa-climate.org/; NDVI, https://modis.gsfc.nasa.gov; GDP, https://figshare.com; NLT, https://zenodo.org/records/7612389; Population density, https://hub.worldpop.org/; Road density, https://www.globio.info; Topographic data, https://www.earthdata.nasa.gov; Biodiversity hotspot dataset, https://zenodo.org/records/3261807; Border port, https://www.openstreetmap.org/; Country classifications by income level, https://www.worldbank.org.

Appendix A. Supplementary material

Supplementary data to this article can be found online at https://doi.org/10.1016/j.scib.2026.01.049.

References

[1] Gong P, Li X, Wang J, et al. Annual maps of global artificial impervious area (GAIA) between 1985 and 2018. Remote Sens Environ 2020;236:111510.

[2] Huang X, Li J, Yang J, et al. 30 m global impervious surface area dynamics and urban expansion pattern observed by Landsat satellites: from 1972 to 2019. Sci China Earth Sci 2021;64:1922–33.
[3] Zhang X, Liu L, Zhao T, et al. GISD30: global 30m impervious-surface dynamic dataset from 1985 to 2020 using time-series Landsat imagery on the Google Earth Engine platform. Earth Syst Sci Data 2022;14:1831–56.
[4] Angel S, Parent J, Civco DL, et al. The dimensions of global urban expansion: estimates and projections for all countries, 2000–2050. Prog Plan 2011;75:53–107.
[5] Gao J, O'Neill BC. Mapping global urban land for the 21st century with data-driven simulations and Shared Socioeconomic Pathways. Nat Commun 2020;11:2302.
[6] Seto KC, Güneralp B, Hutyra LR. Global forecasts of urban expansion to 2030 and direct impacts on biodiversity and carbon pools. Proc Natl Acad Sci USA 2012;109:16083–8.
[7] Grimm NB, Faeth SH, Golubiewski NE, et al. Global change and the ecology of cities. Science 2008;319:756–60.
[8] Li G, Fang C, Li Y, et al. Global impacts of future urban expansion on terrestrial vertebrate diversity. Nat Commun 2022;13:1628.
[9] Qiu L, He J, Yue C, et al. Substantial terrestrial carbon emissions from global expansion of impervious surface area. Nat Commun 2024;15:6456.
[10] van Vliet J, Eitelberg DA, Verburg PH. A global analysis of land take in cropland areas and production displacement from urbanization. Glob Environ Change 2017;43:107–15.
[11] Chen M, Chen L, Cheng J, et al. Identifying interlinkages between urbanization and Sustainable Development Goals. Geogr Sustain 2022;3:339–46.
[12] Xiao C, Li P, Feng Z, et al. Global border watch: from land use change to joint action. Int J Appl Earth Obs Geoinfo 2021;103:102494.
[13] Biggs TW, Atkinson E, Powell R, et al. Land cover following rapid urbanization on the US–Mexico border: implications for conceptual models of urban watershed processes. Landsc Urban Plan 2010;96:78–87.
[14] Soi I, Nugent P. Peripheral urbanism in Africa: border towns and twin towns in Africa. J Borderl Stud 2017;32:535–56.
[15] Rentschler J, Avner P, Marconcini M, et al. Global evidence of rapid urban growth in flood zones since 1985. Nature 2023;622:87–92.
[16] Mahtta R, Fragkias M, Güneralp B, et al. Urban land expansion: the role of population and economic growth for 300+ cities. npj Urban Sustain 2022;2:5.
[17] Li X, Zhou W, Ouyang Z. Forty years of urban expansion in Beijing: what is the relative importance of physical, socioeconomic, and neighborhood factors? Appl Geogr 2013;38:1–10.
[18] Huang Q, Zhang H, van Vliet J, et al. Patterns and distributions of urban expansion in global watersheds. Earths Future 2021;9:e2021EF002062.
[19] Li P, Xiao Z. Impervious surface expansion in the China-Laos border area under the context of geo-economic cooperation: a case study of the Mohan-Boten Economic Cooperation Zone. GIScience Remote Sens 2022;59:2184–201.
[20] Massaro E, Schifanella R, Piccardo M, et al. Spatially-optimized urban greening for reduction of population exposure to land surface temperature extremes. Nat Commun 2023;14:2903.
[21] d'Amour CB, Reitsma F, Baiocchi G, et al. Future urban land expansion and implications for global croplands. Proc Natl Acad Sci USA 2017;114:8939–44.
[22] van Vliet J. Direct and indirect loss of natural area from urban expansion. Nat Sustain 2019;2:755–63.
[23] Cheng Y, Xu Z, Liu H. Sustainable development in global border regions. Science 2024;384:1309.
[24] Vasilijevic M, Zunckel K, Mckinney M, et al. Transboundary conservation: a systematic and integrated approach; 2015. https://iucn.org/resources/publication/transboundary-conservation-systematic-and-integrated-approach.
[25] Yue Z, Xiao C, Feng Z, et al. Accelerating decline of habitat quality in Chinese border areas. Resour Conserv Recycl 2024;206:107665.
[26] Song X-P, Hansen MC, Stehman SV, et al. Global land change from 1982 to 2016. Nature 2018;560:639–43.
[27] Winkler K, Fuchs R, Rounsevell M, et al. Global land use changes are four times greater than previously estimated. Nat Commun 2021;12:2501.
[28] Xiao C, Wang Y, Feng Z, et al. Global cropland loss at borders contributes to increased biodiversity. Commun Earth Environ 2025;6:957.
[29] Lindenmayer D, Scheele BC, Lavery T, et al. Biodiversity response to rapid successive land cover conversions in human-dominated landscapes. Glob Ecol Conserv 2023;45:e02510.
[30] Seifollahi-Aghmiuni S, Kalantari Z, Egidi G, et al. Urbanisation-driven land degradation and socioeconomic challenges in peri-urban areas: insights from Southern Europe. Ambio 2022;51:1446–58.
[31] Luan W, Li X. Rapid urbanization and its driving mechanism in the Pan-Third Pole region. Sci Total Environ 2021;750:141270.
[32] Seto KC, Fragkias M, Güneralp B, et al. A meta-analysis of global urban land expansion. PLOS One 2011;6:1–9.
[33] Zhou L, Dang X, Mu H, et al. Cities are going uphill: slope gradient analysis of urban expansion and its driving factors in China. Sci Total Environ 2021;775:145836.
[34] Baier SL, Bergstrand JH, Feng M. Economic integration agreements and the margins of international trade. J Int Econ 2014;93:339–50.
[35] de Medeiros CA, Mazat N. Geopolitics, geoeconomics, and development strategies in the new millennium. In: Fernández VR, Brondino G, editors. Development in Latin America. Cham: Palgrave Macmillan; 2019. p. 89–122.
[36] Xiao C, Wang Y, Yan M, et al. Impact of cross-border transportation corridors on changes of land use and landscape pattern: a case study of the China-Laos railway. Landsc Urban Plan 2024;241:104924.
[37] Kim KC. Preserving biodiversity in Korea's demilitarized zone. Science 1997;278:242–3.
[38] Golunov S. The border zone. Russ Polit Law 2013;51:59–70.
[39] Shneiderman S. Himalayan border citizens: sovereignty and mobility in the Nepal–Tibetan Autonomous Region (TAR) of China border zone. Polit Geogr 2013;35:25–36.
[40] Hawes D. Borders and border regions in europe: changes, challenges and chances. J Contemp Eur Stud 2014;22:533–4.
[41] Flesch AD, Epps CW, Cain III JW, et al. Potential effects of the United States-Mexico border fence on wildlife. Conserv Biol 2010;24:171–81.
[42] Xiao C, Feng Z, You Z, et al. Population boom in the borderlands globally. J Clean Prod 2022;371:133685.
[43] Dorigo W, Wagner W, Albergel C, et al. ESA CCI Soil Moisture for improved Earth system understanding: state-of-the art and future directions. Remote Sens Environ 2017;203:185–215.
[44] Myers N, Mittermeier RA, Mittermeier CG, et al. Biodiversity hotspots for conservation priorities. Nature 2000;403:853–8.
[45] Rasmussen C, Williams C. In: Gaussian processes for machine learning. Cambridge: The MIT Press; 2005. p. 1–247.
[46] Gao B, Yang J, Chen Z, et al. Causal inference from cross-sectional earth system data with geographical convergent cross mapping. Nat Commun 2023;14:5875.
[47] Sugihara G, May R, Ye H, et al. Detecting causality in complex ecosystems. Science 2012;338:496–500.
[48] Deng X, Yu W, Shi J, et al. Characteristics of surface urban heat islands in global cities of different scales: trends and drivers. Sustain Cities Soc 2024;107:105483.
[49] Yuan W, Zheng Y, Piao S, et al. Increased atmospheric vapor pressure deficit reduces global vegetation growth. Sci Adv 2019;5:eaax1396.
[50] Lundberg SM, Erion G, Chen H, et al. From local explanations to global understanding with explainable AI for trees. Nat Mach Intell 2020;2:56–67.
[51] Chen T, Guestrin C. XGBoost: a scalable tree boosting system. In: Proceedings of 22nd ACM SIGKDD international conference on knowledge discovery and data mining. Association for Computing Machinery; 2016. p. 785–94.
[52] O'Brien RM. A caution regarding rules of thumb for variance inflation factors. Qual Quant 2007;41:673–90.
[53] Lundberg SM, Lee S-I. A unified approach to interpreting model predictions. In: Proceedings of the 31st international conference on neural information processing systems. Curran Associates Inc.; 2017. p. 4768–77.
[54] Mittakola RT, Ciais P, Schubert JE, et al. Drivers of natural gas use in U.S. residential buildings. Sci Adv 2024;10:eadh5543.
[55] Aas K, Jullum M, Løland A. Explaining individual predictions when features are dependent: more accurate approximations to Shapley values. Artif Intell 2021;298:103502.
[56] Carlsson LS, Samuelsson PB, Jönsson PG. Interpretable machine learning—tools to interpret the predictions of a machine learning model predicting the electrical energy consumption of an electric arc furnace. Steel Res Int 2020;91:2000053.
[57] Chakraborty S, Maity I, Dadashpoor H, et al. Building in or out? Examining urban expansion patterns and land use efficiency across the global sample of 466 cities with million+ inhabitants. Habitat Int 2022;120:102503.
[58] Colsaet A, Laurans Y, Levrel H. What drives land take and urban land expansion? A systematic review. Land Use Policy 2018;79:339–49.
[59] Su P, Grydehøj A. Bordered and crossborder perspectives on sustainable development: spatial planning in Hengqin, China. Cities 2024;150:105014.
[60] Li F, Liu H, Huisingh D, et al. Shifting to healthier cities with improved urban ecological infrastructure: from the perspectives of planning, implementation, governance and engineering. J Clean Prod 2017;163:S1–S11.
[61] Cabral AIR, Costa FL. Land cover changes and landscape pattern dynamics in Senegal and Guinea Bissau borderland. Appl Geogr 2017;82:115–28.
[62] McDonald RI, Mansur AV, Ascensão F, et al. Research gaps in knowledge of the impact of urban growth on biodiversity. Nat Sustain 2020;3:16–24.
[63] Müller MF, Yoon J, Gorelick SM, et al. Impact of the Syrian refugee crisis on land use and transboundary freshwater resources. Proc Natl Acad Sci USA 2016;113:14932–7.
[64] Halkos GE, Tsilika KD. Understanding transboundary air pollution network: emissions, depositions and spatio-temporal distribution of pollution in European region. Resour Conserv Recycl 2019;145:113–23.
[65] Simkin RD, Seto KC, McDonald RI, et al. Biodiversity impacts and conservation implications of urban land expansion projected to 2050. Proc Natl Acad Sci USA 2022;119:e2117297119.
[66] Chen X, Hull V. Border conservation in Hindu Kush-Himalaya. Science 2023;380:1330–2.
[67] Liu J, Yong DL, Choi C-Y, et al. Transboundary frontiers: an emerging priority for biodiversity conservation. Trends Ecol Evol 2020;35:679–90.
[68] Heimberger P. Does economic globalisation affect income inequality? A meta-analysis. World Econ 2020;43:2960–82.
[69] Blum R, Boyden J. Understand the lives of youth in low-income countries. Nature 2018;554:435–7.
[70] Kalliovirta L, Malinen T. Non-linearity and cross-country dependence of income inequality. Rev Income Wealth 2020;66:227–49.

[71] Poumanyvong P, Kaneko S, Dhakal S. Impacts of urbanization on national transport and road energy use: evidence from low, middle and high income countries. Energy Policy 2012;46:268–77.
[72] Dayton L. How South Korea made itself a global innovation leader. Nature 2020;581:S54–6.
[73] Wilkinson RG, Pickett KE. Why the world cannot afford the rich. Nature 2024;627:268–70.
[74] Khan MS. Absorptive capacities approaches for investigating national innovation systems in low and middle income countries. Int J Innov Stud 2022;6:183–95.
[75] de Siqueira Filha NT, Li J, Phillips-Howard PA, et al. The economics of healthcare access: a scoping review on the economic impact of healthcare access for vulnerable urban populations in low- and middle-income countries. Int J Equity Health 2022;21:191.
[76] Moallemi EA, Malekpour S, Hadjikakou M, et al. Achieving the sustainable development goals requires transdisciplinary innovation at the local scale. One Earth 2020;3:300–13.
[77] Röder A, Pröpper M, Stellmes M, et al. Assessing urban growth and rural land use transformations in a cross-border situation in Northern Namibia and Southern Angola. Land Use Policy 2015;42:340–54.
[78] Perkmann M, Sum N-L. Globalization, regionalization and cross-border regions: scales, discourses and governance. In: Perkmann M, Sum N-L, editors. Globalization, Regionalization and Cross-Border Regions. London: Palgrave Macmillan UK; 2002. p. 3–21.
[79] Sohn C. Modelling cross-border integration: the role of borders as a resource. Geopolitics 2014;19:587–608.
[80] Lisa P, Christian L, Karen B, et al. Armed conflict and cross-border asymmetries in urban development: a contextualized spatial analysis of Goma, Democratic Republic of the Congo and Gisenyi, Rwanda. Land Use Policy 2021;109:105711.
[81] Pupier P. Spatial evolution of cross-border regions. Contrasted case studies in North-West Europe. Eur Plan Stud 2020;28:81–104.
[82] Song T, Cheng Y, Liu W, et al. Spatial difference and mechanisms of influence of geo-economy in the border areas of China. J Geogr Sci 2017;27:1463–80.
[83] Wang Y, Xiao C. Spatiotemporal characteristics and the national variations of borderland use change in Laos within the geopolinomical context. Front For Glob Change 2023;6:1223605.
[84] McAusland C, Millimet DL. Do national borders matter? Intranational trade, international trade, and the environment. J Environ Econ Manag 2013;65:411–37.
[85] Nienaber B, Wille C. Cross-border cooperation in Europe: a relational perspective. Eur Plan Stud 2020;28:1–7.
[86] Pereira HM, Martins IS, Rosa IMD, et al. Global trends and scenarios for terrestrial biodiversity and ecosystem services from 1900 to 2050. Science 2024;384:458–65.
[87] de Lima RAF, Dauby G, de Gasper AL, et al. Comprehensive conservation assessments reveal high extinction risks across Atlantic Forest trees. Science 2024;383:219–25.